

Momentum matching in the tunneling between 2-dimensional and 0-dimensional electron systems

Andreas Beckel, Daming Zhou, Bastian Marquardt, Dirk Reuter, Andreas D. Wieck et al.

Citation: *Appl. Phys. Lett.* **100**, 232110 (2012); doi: 10.1063/1.4728114

View online: <http://dx.doi.org/10.1063/1.4728114>

View Table of Contents: <http://apl.aip.org/resource/1/APPLAB/v100/i23>

Published by the [American Institute of Physics](http://www.aip.org).

Related Articles

Observation of a Coulomb blockade in strontium titanate thin films

Appl. Phys. Lett. **100**, 203110 (2012)

Tunneling resistance and its effect on the electrical conductivity of carbon nanotube nanocomposites

J. Appl. Phys. **111**, 093726 (2012)

Rashba spin-orbit effect on tunneling time in graphene superlattice

J. Appl. Phys. **111**, 093724 (2012)

Gate-controlled spin transport in a spin-diode structure

J. Appl. Phys. **111**, 093717 (2012)

Tunneling conductivity in composites of attractive colloids

J. Chem. Phys. **136**, 164903 (2012)

Additional information on *Appl. Phys. Lett.*

Journal Homepage: <http://apl.aip.org/>

Journal Information: http://apl.aip.org/about/about_the_journal

Top downloads: http://apl.aip.org/features/most_downloaded

Information for Authors: <http://apl.aip.org/authors>

ADVERTISEMENT



AIP Advances

Special Topic Section:
PHYSICS OF CANCER

Why cancer? Why physics? [View Articles Now](#)

Momentum matching in the tunneling between 2-dimensional and 0-dimensional electron systems

Andreas Beckel,¹ Daming Zhou,^{1,(a)} Bastian Marquardt,¹ Dirk Reuter,² Andreas D. Wieck,² Martin Geller,¹ and Axel Lorke¹

¹Fakultät für Physik and CENIDE, Universität Duisburg-Essen, Lotharstraße 1, 47048 Duisburg, Germany

²Lehrstuhl für Angewandte Festkörperphysik, Ruhr-Universität Bochum, Universitätsstraße 150, 44780 Bochum, Germany

(Received 20 April 2012; accepted 23 May 2012; published online 7 June 2012)

We investigate the tunneling rates from a 2-dimensional electron gas (2DEG) into the ground state of self-assembled InGaAs quantum dots. These rates are strongly affected by a magnetic field perpendicular to the tunneling direction. Surprisingly, we find an increase in the rates for fields up to 4 T before they decrease again. This can be explained by a mismatch between the characteristic momentum of the quantum dot ground state and the Fermi momentum k_F of the 2DEG. Calculations of the tunneling probability can account for the experimental data and allow us to determine the dot geometry as well as k_F . © 2012 American Institute of Physics.

[<http://dx.doi.org/10.1063/1.4728114>]

The interaction between tunable, localized charges and a two-dimensional electron channel is of great technological importance as it is the basis of today's non-volatile flash memory devices. At the same time, the controlled manipulation of charge in low-dimensional semiconductor systems¹ has been an active field of basic research, because it is a promising route for large scale integration of quantum information storage and manipulation.^{2,3} Combining both aspects, self-assembled quantum dots (QDs), embedded in the dielectric of a field-effect transistor structure, have been proposed as a next-generation non-volatile memory device.^{4,5} Here, we investigate the tunneling between a layer of self-assembled InAs quantum dots and a two-dimensional electron gas (2DEG). A recently developed pulse technique makes it possible to directly determine the tunneling rate.^{6,7} A magnetic field applied perpendicular to the tunneling direction (i.e., in the plane of the 2DEG) allows us to shift the momentum of the tunneling electrons.^{8–14} We observe a distinct maximum in the tunneling rate when the magnetic-field-induced shift matches the momentum of the 2D carriers at the Fermi energy, similar to tunneling in 2D-2D systems with unequal carrier densities.^{8,15,16} Model calculations, taking into account the momentum distribution of both the quantum dots and the 2DEG, can very well reproduce the experimental data. This makes it possible to obtain detailed information on the wave function in the quantum dots, such as their characteristic length and their anisotropy.

The investigated samples were grown by solid source molecular-beam epitaxy. On a semi-insulating GaAs(001) substrate, a 360 nm buffer layer and an inverted high electron mobility transistor were deposited. The latter consists of 300 nm Al_{0.34}Ga_{0.66}As, a Si delta doping layer, followed by a 16 nm Al_{0.34}Ga_{0.66}As spacer layer and a 15 nm GaAs quantum well. Subsequently, 10 nm Al_{0.34}Ga_{0.66}As and 5 nm GaAs were grown as a tunneling barrier. For the quantum

dots, approximately 1.9 ML InAs were deposited at 525 °C and covered with 30 nm GaAs. Growth of a 116 nm thick GaAs/AlAs superlattice blocking layer and a 5 nm thick cap layer completed the heterostructure. Samples of 4 × 4 mm² were cleaved from the wafer and patterned into transistor structures (Fig. 1(a)), using optical lithography and wet chemical etching. Ohmic source and drain contacts were fabricated by annealing Ni/AuGe/Au layers, and Ti/Au was deposited as a gate electrode. The active gate area comprises about 8 × 10⁵ QDs. The samples were mounted in a liquid He cryostat equipped with a superconducting solenoid, allowing magnetic fields of $-12 \text{ T} \leq B \leq 12 \text{ T}$ to be applied parallel to the epitaxial layers. In particular, two crystal orientations, $B \parallel (110)$ and $B \parallel (1\bar{1}0)$, were investigated, as these are the main symmetry axes of the (anisotropic) quantum dots.¹¹ The conductivity of the 2D channel was measured by applying a constant voltage of $V_{SD} = 8 \text{ mV}$ along the electron channel and measuring the resulting current with a sampling rate of 125 kHz. Transconductance spectroscopy measurements were performed as described elsewhere⁶ in order to identify the gate voltages at which the quantum dots become occupied with 1...6 electrons each.

Figure 1(b) shows the response of the 2DEG conductivity σ when a rectangular voltage pulse $\Delta V_G = 20 \text{ mV}$ is applied to the gate at a time $t = 0$. Here, the starting gate bias of $V_G(t < 0) = -0.67 \text{ V}$ is chosen, because it corresponds to the charging of the first electron into the dots for the average-sized quantum dot in the ensemble. Around $t = 0$, the conductivity of the 2DEG abruptly rises, as its carrier density increases, following the (positive) gate voltage pulse. The subsequent drop in σ is caused by a gradual decrease of the 2D carrier density as some of the electrons tunnel through the barrier and occupy empty dot states.⁵ We find that for tunneling into the quantum dot ground state ("s-state"), the time dependence of the conductivity can be described by an exponential decay, $\Delta\sigma(t) = \Delta\sigma_0 e^{-t/\tau}$, see inset in Fig. 1(b). This allows us to directly determine the time constant τ and the tunneling rate $1/\tau$, respectively, between the 2DEG and the quantum dots.

^(a)On leave from Shanghai Advanced Research Institute, Chinese Academy of Sciences, No. 99 Haike Road, Zhangjiang Hi-Tech Park, Pudong, Shanghai 201203, China.

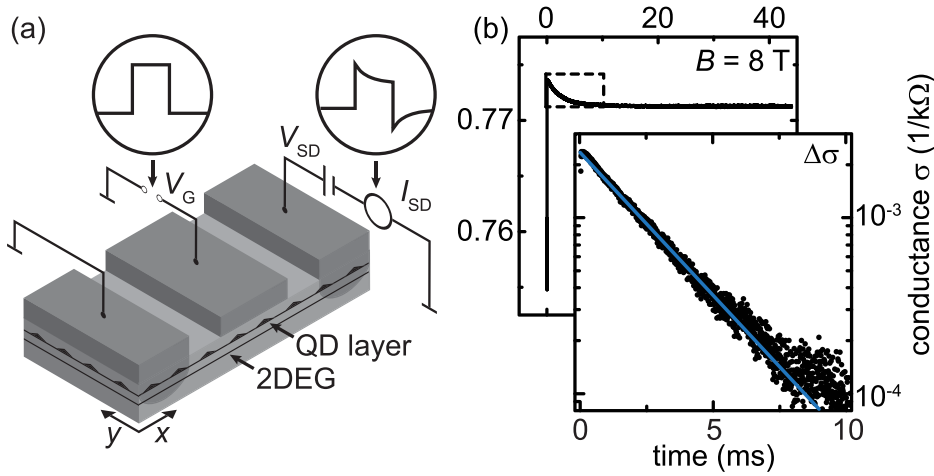


FIG. 1. (a) Schematic of the sample layout and the measurement configuration. (b) Time resolved response of the 2DEG conductance, when a rectangular pulse V_G is applied to the gate. The slow decay corresponds to the tunneling transfer of charge to the quantum dots. It roughly follows an exponential decay (see inset), which is given by the tunneling rate.

The data points in Fig. 2 summarize the thus obtained tunneling rates $1/\tau$ as a function of B_{\parallel} , applied along the two orthogonal directions (Fig. 2, top and bottom). Contrary to previous studies which used highly doped bulk (3D) back contacts,^{9–11,13} we observe that the tunneling rate into the lowest dot state *increases* with increasing magnetic field up to $B_{\parallel} \approx 4.5$ T.

This indicates a fundamental difference in the magneto-tunneling spectroscopy of coupled 2D–0D systems, compared to 3D–0D systems. In samples with a 3D emitter, tunneling is dominated by states with $k_{\parallel} = 0$ or, in other words, by states, which impinge perpendicularly onto the tunneling barrier with maximum k_z (z is the tunneling direction, (001), and k_{\parallel} is the momentum in the (x, y) plane).¹⁰ For coupled 2D–0D systems, on the other hand, k_z is fixed by the quantum confine-

ment of the 2DEG and k_{\parallel} is given by its Fermi wave vector $k_{\parallel} = k_F = \sqrt{2\pi n_s}$, where n_s is the 2D carrier density. Because the maximum of the s -state wave function in the dot is at $k_{\parallel} = 0$, tunneling between the 2D emitter and the quantum dots will be reduced by the corresponding momentum mismatch. This is illustrated in inset (a) of Fig. 2, where the wave function of the dot is plotted schematically in k -space and compared to the Fermi circle of the 2DEG. For a sufficiently large k_F , the overlap between the Fermi circle and the wave function of the dot will be small and tunneling will be reduced accordingly. When an in-plane magnetic field B_{\parallel} is applied, the momentum of the emitted electrons will shift by an amount^{8,9} $\Delta k = eB_{\parallel}\Delta z/\hbar$, where Δz is the tunneling distance between the emitter and the dots (see inset (b) and (c)). Therefore, with increasing field, the wave function overlap will first increase, until it reaches a maximum at $\Delta k \approx k_F$ (inset (b)). When the magnetic field is increased even further, the overlap between dot and 2DEG wave function will decrease again, as schematically depicted in inset (c). This is all in qualitative agreement with the experimental findings.

For a more in-depth evaluation of the data, we follow the approach in Refs. 10 and 14 and calculate the overlap integral of the wave functions in the 2DEG and the quantum dots $|\langle \Psi_{2\text{DEG}} | \Psi_{\text{QD}} \rangle|^2$. First, we need to address how B_{\parallel} affects the electron states in the emitter. Without loss of generality, we take $B_{\parallel} = (B, 0, 0)$ and use the Landau gauge $A = (0, -Bz, 0)$. Straightforward solution of the resulting Schrödinger equation¹⁷ yields

$$E = E_z^* + \frac{\hbar^2}{2m} \left(k_x^2 + k_y^2 \frac{E_z^*}{E_z^{*2}} \right), \quad (1)$$

where E_z^* is the diamagnetically shifted and E_z the bare confinement energy of the quantum well. In the present situation, where E_z is much larger than the cyclotron energy, we find $E_z^* \approx E_z$, and Eq. (1) reduces to the usual dispersion of a 2D free electron gas. Similar arguments also apply to the states in the quantum dots, so that the parallel magnetic field essentially only affects the tunneling process by the above-mentioned momentum shift Δk .

For the quantum dot states we use the now well-established model of parabolic confinement,^{14,18} which gives

$$\psi_{\text{QD}} = \sqrt{\frac{k_x k_y}{\pi}} e^{-\frac{1}{2}(k_x^2 x^2 + k_y^2 y^2)} \quad (2)$$

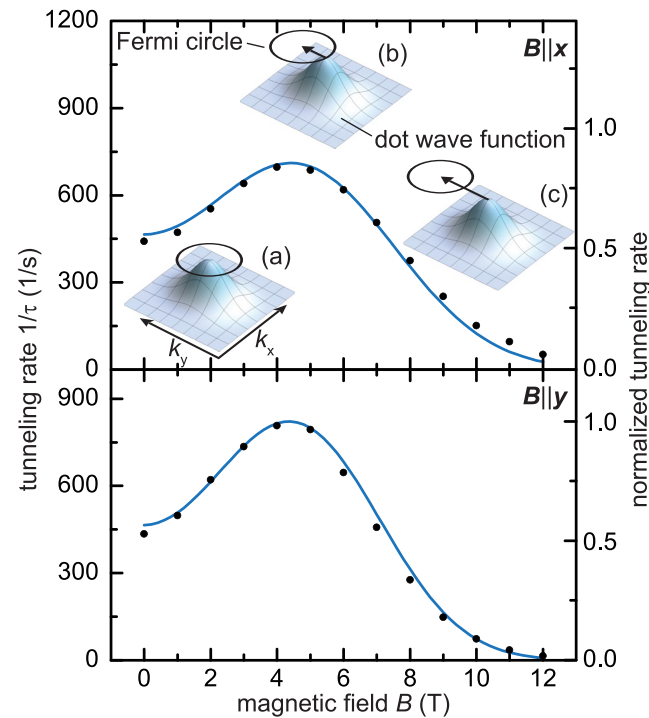


FIG. 2. Data points measured tunneling rate as a function of magnetic field for two orthogonal field directions (top and bottom). Lines are calculated probabilities for dot dimensions $L_x = 8.0$ nm, $L_y = 6.8$ nm, and Fermi wave vector $k_F = 0.19$ nm⁻¹. Insets indicate how the Fermi circle lines up with the dot wave function for (a) vanishing field, (b) intermediate fields, and (c) high fields. Optimum momentum matching is achieved when the shift approximately equals k_F (b).

as the ground state wave function, with k_x and k_y being the characteristic momentum (inverse characteristic length) of the parabolic dot potential along the (110) and the (110) directions. Following the discussion above, the emitter wave functions are taken to be plane waves of momentum k_F . The overlap integral is calculated numerically and summed up over the Fermi circle, which is displaced by Δk as a result of the in-plane magnetic field.

In order to calculate the shift in momentum, $\Delta k = eB_{\parallel}\Delta z/\hbar$, the tunneling distance Δz is needed, which is larger than the geometric width of the tunneling barrier (15 nm), because the maximum of the wave function in the back contact is shifted away from the GaAs/(AlGa)As interface. To estimate the tunneling distance, we solve the 1D Schrödinger and Poisson equations for the given heterostructure¹⁹ and find that the calculated maximum of the charge carrier density is shifted by 9 nm from the interface towards the substrate. This results in a tunneling distance of $\Delta z = 24 \pm 1$ nm, which is then used to calculate the displacement in k-space for the overlap integrals.

The lines in Fig. 2 show the results of our model calculation for $k_F = 1.9 \times 10^8 \text{ m}^{-1}$, which corresponds to a 2D carrier density of $n_s = 6 \times 10^{11} \text{ cm}^{-2}$ obtained by Hall measurements and characteristic lengths $L_x = 1/k_x = 8.0$ nm, $L_y = 1/k_y = 6.8$ nm. It can be seen that all experimental data points can be very well reproduced. The comparison between the detailed calculations and the experimental data thus allows us to determine the spatial confinement of the wave function in the dot as well as the Fermi wave vector in the 2D back contact. Because the entire Fermi circle enters the calculation, the values for L_x and L_y affect the calculated results for both magnetic field orientations. In this context, we would like to discuss the accuracy of our assumption of a circular Fermi surface. Indeed, on standard (triangular well) heterostructures, distortions of the Fermi circle²⁰ of 5%–10% have been observed in parallel magnetic fields of ≈ 6 T.^{20,21} Since the distortion is quadratic in the confinement energy (see Eq. (1)) and in the present experiment E_z is much larger than in standard heterostructures, we estimate the error from this approximation to be only a few percent.

Therefore, the good agreement between experiment and calculation strongly supports our conclusion that the non-monotonic behavior of the magnetotunneling rates seen in Fig. 2 is indeed caused by the momentum mismatch of the 2DEG and the dots.

Our findings may open up a new route for the electrical control of the tunneling probability in epitaxial systems, where the tunneling barrier itself is not tunable. When the 2D carrier density can be independently set, e.g., by the application of an additional back gate, the diameter of the Fermi circle becomes adjustable. This in turn will affect the momentum mismatch, so that the tunneling rate can be controlled by the applied bias.

Furthermore, we believe that the present method to obtain the dimensions L_x and L_y of the dot wave function is of high accuracy, since it starts from a direct measurement of the tunneling time (see Fig. 1(b)) rather than from an evaluation of the capacitive tunneling current. Indeed, our present experimental results lead to considerably larger dot dimen-

sions L_x, L_y (smaller characteristic momenta k_x and k_y) than the data from capacitance spectroscopy, in agreement with theoretical results.¹³

In summary, we have shown that a momentum mismatch can strongly affect the tunneling between 2-dimensional and 0-dimensional electron systems. For sufficiently high 2D carrier densities, tunneling into the ground state of self-assembled dots can be considerably suppressed. The application of a magnetic field perpendicular to the tunneling direction can be used to offset the momentum mismatch and increase the tunneling rate. A detailed comparison between the experimental magnetotunneling rates and calculations of the wave function overlap makes it possible to determine both the spatial extent of the dots' ground state and the Fermi wave vector in the 2D electron system. Our results open up new possibilities to control the coherent transport in semiconductor quantum structures.

We acknowledge financial support by the Mercator Research Center Ruhr (MERCUR) of Stiftung Mercator and the DFG (Contract No. GE 2141/1-1) in the framework of the NanoSci-E+ project QD2D of the European Commission. D. Zhou would like to thank the China Scholarship Council (CSC) for financial support.

- ¹See, e.g., S. Reimann and M. Manninen, *Rev. Mod. Phys.* **74**, 1283 (2002).
- ²D. Loss and D. P. DiVincenzo, *Phys. Rev. A* **57**, 120 (1998).
- ³T. D. Ladd, F. Jelezko, R. Laflamme, Y. Nakamura, C. Monroe, and J. L. O'Brien, *Nature (London)* **464**, 45 (2010).
- ⁴S. Tiwari, F. Rana, H. Hanafi, A. Hartstein, E. F. Crabbé, and K. Chan, *Appl. Phys. Lett.* **68**, 1377 (1996).
- ⁵A. Marent, M. Geller, A. Schliwa, D. Feise, K. Pötschke, N. Akcay, N. Öncan, and D. Bimberg, *Appl. Phys. Lett.* **91**, 242109 (2007).
- ⁶B. Marquardt, M. Geller, A. Lorke, D. Reuter, and A. D. Wieck, *Appl. Phys. Lett.* **95**, 022113 (2009).
- ⁷B. Marquardt, M. Geller, B. Baxevanis, D. Pfannkuche, A. D. Wieck, D. Reuter, and A. Lorke, *Nat. Commun.* **2**, 209 (2011).
- ⁸J. Smoliner, W. Demmerle, G. Berthold, E. Gornik, and G. Weimann, *Phys. Rev. Lett.* **63**, 2116 (1989).
- ⁹E. Vdovin, A. Levin, A. Patane, L. Eaves, P. Main, Y. Khanin, Y. Dubrovskii, M. Henini, and G. Hill, *Science* **290**, 122 (2000).
- ¹⁰A. Patane, R. Hill, L. Eaves, P. Main, M. Henini, M. Zambrano, A. Levin, N. Mori, C. Hamaguchi, Y. Dubrovskii, E. Vdovin, D. Austing, S. Tarucha, and G. Hill, *Phys. Rev. B* **65**, 165308 (2002).
- ¹¹O. Wibbelhoff, A. Lorke, D. Reuter, and A. Wieck, *Appl. Phys. Lett.* **86**, 092104 (2005); O. Wibbelhoff, A. Lorke, D. Reuter, and A. Wieck, *ibid.* **88**, 129901 (2006).
- ¹²M. Rontani and E. Molinari, *Phys. Rev. B* **71**, 233106 (2005).
- ¹³G. Bester, D. Reuter, L. He, A. Zunger, P. Kailuweit, A. D. Wieck, U. Zeitler, J. C. Maan, O. Wibbelhoff, and A. Lorke, *Phys. Rev. B* **76**, 075338 (2007).
- ¹⁴W. Lei, C. Notthoff, J. Peng, D. Reuter, A. Wieck, G. Bester, and A. Lorke, *Phys. Rev. Lett.* **105**, 176804 (2010).
- ¹⁵J. P. Eisenstein, T. J. Gramila, L. N. Pfeiffer, and K. W. West, *Phys. Rev. B* **44**, 6511 (1991).
- ¹⁶A. Kurobe, I. M. Castleton, E. H. Linfield, M. P. Grimshaw, K. M. Brown, D. A. Ritchie, M. Pepper, and G. A. C. Jones, *Phys. Rev. B* **50**, 4889 (1994).
- ¹⁷For simplicity and to allow for an analytical solution, we have assumed a parabolic confinement of the 2DEG along the z-direction.
- ¹⁸R. Warburton, B. Miller, C. Dürr, C. Bödefeld, K. Karrai, J. Kotthaus, G. Medeiros Ribeiro, P. Petroff, and S. Huan, *Phys. Rev. B* **58**, 16221 (1998).
- ¹⁹G. L. Snider, *Computer Program 1D POISSON/SCHRÖDINGER: A Band Diagram Calculator*, University of Notre Dame, Notre Dame, Indiana. See also www.nd.edu/~gsnider.
- ²⁰L. Smrcka and T. Jungwirth, *J. Phys.: Condens. Matter* **6**, 55 (1994).
- ²¹K. Ohtsuka, S. Takaoka, K. Oto, K. Murase, and K. Gamo, *Physica B* **251**, 780 (1998).